

NUMERICAL SIMULATION ON THE AERODYNAMIC FORCE OF THE ICED CONDUCTOR FOR DIFFERENT ANGLES OF ATTACK

Y. Liu* – A. P. Tang, – K. T. Liu – J. W. Tu

School of civil Engineering, Harbin Institute of technology, Harbin, Heilongjiang province, China

ARTICLE INFO

Article history:

Received: 19.06.2014.

Received in revised form: 06.11.2014.

Accepted: 11.11.2014.

Keywords:

Galloping

Aerodynamic force

Iced conductor

Vortex shedding

Den Hartog mechanism

O.Nigol mechanism

Abstract:

According to the galloping mechanism of iced conductors, the aerodynamic simulations were performed based on actual wind tunnel tests. Aeroelastic models of single and bundled conductors with a typical ice-coating section forms (crescent section) were set up. The simulation results were in good agreements with wind tunnel tests, and it showed that numerical simulation method can be used instead of wind tunnel tests. The wind attack angles have seriously affected the aerodynamic force of the iced conductor. The wake of vortex shedding for the iced single conductor was analyzed. As for the iced bundled conductors, sub-conductors at the downstream were seriously influenced by the ones at the upstream locations, and the aerodynamic force of the sub-conductors at the downstream was lower than of those at the upstream. The negative slope of Nigol coefficient to the bundled conductors was larger than that of the single wire, but the absolute value of the amplitude was less than that of the single conductor, and the bundled conductors were more likely to gallop than the single ones. The Den. Hartog and O.Nigol mechanism were used to predict galloping of iced conductors, which can be convenient for analyzing vibration of iced conductors.

1 Introduction

The construction of transmission lines has made a great progress with the development of national economy. Power transmission projects become more and more complicated by increasing the voltage level, transmission towers are higher and

the span of lines becomes larger than ever before. Due to the development of power grids interconnection and bad weather, the possibility of complex power system faults will be increased. A wide range of galloping motions happen almost not only every year in power supply systems in Northern China, but these events have also occurred

*Corresponding author. Tel.: +8613904601224;
E-mail: liuyuejun123456@126.com

for many years. The further study on anti-galloping is very important for the transmission line safety and sustainable development.

The research of galloping began in the early 1930s, and since then many scholars have done a lot of tests and theoretical researches on galloping. O. Chabart et al. [1] studied galloping generated during wind tunnel testing and reproduced a typical eccentric ice shape on a classical stranded overhead transmission conductors, and the quasi-static aerodynamic coefficients have been measured for different wind speeds. Zhitao Yan et al.[2-3] explored the galloping of single and bundled iced conductors based on the displacement interpolations and curvature-displacement relationship of spatial curved-beam theory; subsequently a finite element model of iced conductor galloping was presented involving 3 translational and 3 rotational degrees of freedom. A.M. Loredo-Souza et al. [4] developed a new modeling approach to conductor systems using a distorted horizontal length scale, were concerned with the behaviour of transmission lines in severe boundary layer wind, and examined the scale of turbulence on the response of cable structure through wind tunnel tests. Qiang Xie et al. [5] carried out a series of wind tunnel experiments to measure the global drag coefficients of multi-bundled conductors with the conductor diameter, bundle number, wind turbulence intensity and wind attack angle. Pierre Van Dykea et al. [6] conducted galloping measurements on a high-voltage overhead test line equipped with a single conductor as well as a second configuration of three conductors with interphase spacers. Galloping was induced by using D-sections over the conductor. Wind azimuth strongly influenced the galloping amplitude. A.M. Loredo-Souza et al. [7] examined the behaviours of two parallel transmission line cables under high wind through aeroelastic wind tunnel testing of cable models. Correlation coefficients representing drag forces of the two cables were obtained, which varied little with wind velocity and were bigger for the smallest separation between cables.

A set of programs for galloping simulation of the transmission lines developed by Guo Yinglong et al. [8-9], was also relatively completed. Li Wanping et al. [10] did the wind tunnel test to study the aerodynamic characteristics of single and bundled conductors. The aerodynamic characteristics of iced conductors were theoretical basis for preventing galloping. The Den. Hartog vertical mechanism and

O.Nigol torsional mechanism were put forward successively.

2 The galloping mechanism of iced transmission lines

2.1 Vertical galloping mechanism

Galloping mechanism of cross-wind direction (Den. Hartog mechanism [11]) is the most representative galloping excitation mechanism. Considering the iced conductor with a crescent section which produced eccentric load, and the wind force on the conductors which was decomposed into horizontal and vertical forces, Den. Hartog proposed the necessary conditions of galloping instability as follows(Eq.1).

$$\delta_D = C_D + \frac{\partial C_L}{\partial \alpha} < 0, \quad (1)$$

where, δ_D is the coefficient of Den. Hartog; C_L is the lift coefficient; C_D is the drag coefficient; α is the attack angle in degrees.

The iced conductor had an irregular shape, large amplitude vibrations were caused by lift and drag interchange. Den. Hartog researched the aerodynamic characteristics of an eccentric iced conductor but ignored the influence of the torsion.

2.2 Torsional galloping mechanism

O.Nigol[12-13] considered overhead transmission lines that were not only moved up and down, but had a twist as well. Galloping would happen when frequency of transverse vertical vibration was equal to the torsional frequency of transmission line. The necessary conditions of galloping instability were given as (Eq.2):

$$\delta_N = \frac{\partial C_M}{\partial \alpha} < 0, \quad (2)$$

where δ_N is the coefficient of Nigol; C_M is Moment Coefficient; α is the attack angle in degrees.

3 Numerical simulations on aerodynamic characteristics of an iced single conductor with a crescent section

3.1 Governing equations

In the rectangular coordinate system, N - S equation can be used to describe the motion of incompressible viscous fluid, whose viscosity of the fluid is constant. Although the continuity equation, momentum equation and energy equation are the basic equations of the fluid flow and heat transfer, for incompressible flow however, heat exchange is so small that the energy equation can be ignored since it does not need to consider the energy conservation equation. Therefore, it is necessary only to solve continuity equation and momentum equations [11]:

Continuity equation (Eq.3):

$$\frac{\partial u}{\partial x} + \frac{\partial w}{\partial z} = 0 \quad (3)$$

Momentum equations(Eq.4,5):

$$\frac{\partial u}{\partial t} + u \frac{\partial u}{\partial x} + w \frac{\partial u}{\partial z} = -\frac{1}{\rho} \frac{\partial p}{\partial x} + \nu \left[\frac{\partial^2 u}{\partial x^2} + \frac{\partial^2 u}{\partial z^2} \right], (4)$$

$$\frac{\partial w}{\partial t} + u \frac{\partial w}{\partial x} + w \frac{\partial w}{\partial z} = -\frac{1}{\rho} \frac{\partial p}{\partial z} + \nu \left[\frac{\partial^2 w}{\partial x^2} + \frac{\partial^2 w}{\partial z^2} \right], (5)$$

where u is a velocity component in x ; w is a velocity component in z ; ρ is the density of the fluid; p is the pressure of the fluid; ν is kinematic viscosity of the fluid.

3.2 Boundary conditions

Figure 1 shows a computational domain and boundary condition. When the wind direction is perpendicular to the boundary of AB, AB is the velocity-inlet. CD is the velocity-outlet, AD and BC are symmetric boundaries, which are the sliding boundaries. If the wind direction has an angle with the boundary of AB, AB and BC are the velocity-inlets, CD and AD are the boundaries of the

outflow. The surface of an iced conductor is the wall, which is called no-sliding boundary. The length from the no-sliding boundary to the outlet is big enough to have no effect on the upstream flow. In this paper, the Turbulence Intensity is set to $I=6\%$, the Turbulent Viscosity Ratio is $R=10$.

3.3 Numerical method

The discretized equations were solved by SIMPLE (Semi Implicit Method for Pressure - Linked Equations) algorithm based on the staggered grid. Second Order Upwind was selected in discrete form, convergence criteria was 10^{-5} . Second-order central difference format was used in the viscous term. SST $k-\omega$ model was selected to simulate turbulence taken into account as turbulent shear stress as SST $k-\omega$ model has a higher precision and greater credibility in a wide range of flow fields.

3.4 Modeling conditions and system configurations

Based on the wind tunnel test for aerodynamic characteristics of iced conductors (Zhejiang University, China) [14], the iced conductor models with crescent sections were simulated by finite element analysis software ANSYS. On the basis of experience, when the galloping happened, the wind speed was usually less than 20 m/s, mostly focused on 7 to 15 m/s. The wind speed in the test was 10 m/s. The influence of turbulent flow should be considered. The Reynolds number can be calculated as follows (Eq.6):

$$Re = UD / \nu \approx (2.4 \sim 3.6) \times 10^4, \quad (6)$$

where, D is the diameter of the conductor, ν is the kinematic viscosity of air.

ACSR (Aluminium Cable Steel Reinforced) LGJ-600/45 was chosen. The diameter of the conductor was 33.6 mm, and 35 mm was chosen in order to create a model conveniently. The ice thickness was 21 mm. The conductor models with crescent sections were combined by a half circle and semi-elliptical. The minor axis of the elliptical was equal to the radius of the conductor, and the major axis was 38.5 mm. Since the ice made the gravity center shift, the model of an iced conductor was established with an angle of 15° . The computational domain was rectangle, the length of the domain was

60D and the width was 30D. As shown in Figure 1, the center of the conductor was placed at the original point, which was 15D, 45D, 15D and 15D from the inlet boundary, outlet boundary, left and right boundary, respectively. The unstructured mesh was used, and the mesh density was higher at the central region of the iced conductor, shown in

Figure 2. The iced conductor with a crescent section assumed symmetrical arrangement. Therefore, there was only the need to monitor the aerodynamic coefficient for the wind attack angle from 0° to 180°, and eventually the attack angle was increased by 5°.

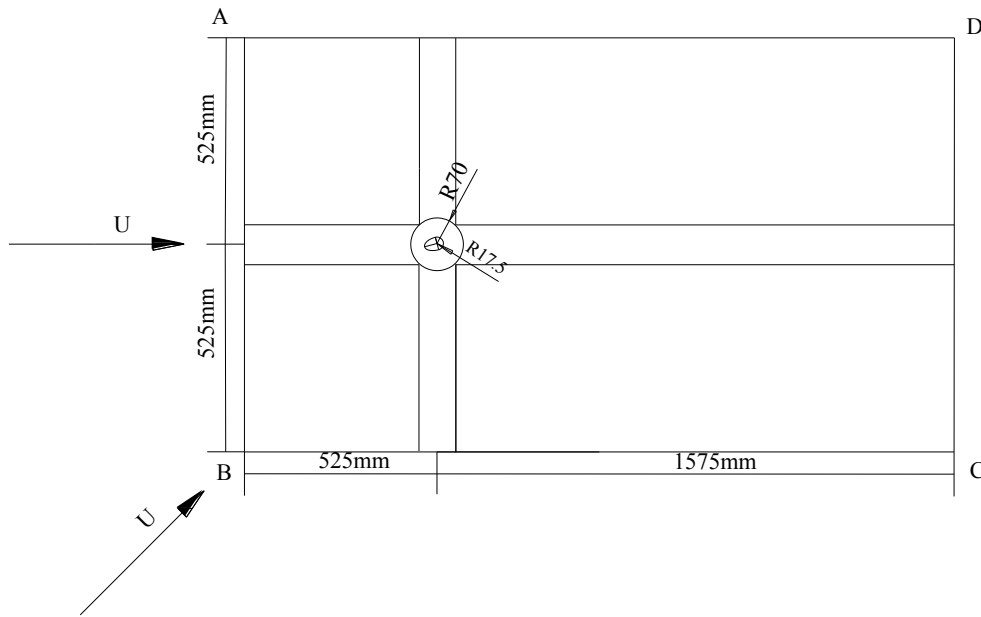


Figure1. Computational domain and boundary condition.

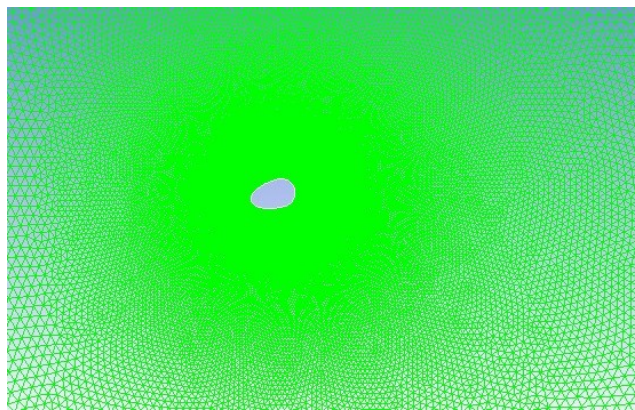


Figure2. The mesh of central region of iced conductor.

3.5 Definitions of aerodynamic coefficients

As shown in Figure 3, the aerodynamic force of the iced conductor produced by the wind was divided into drag F_D , lift F_L , and moment M [15]. Its dimensionless aerodynamic coefficients can be defined as follows(Eq.7-9):

$$C_D = \frac{F_D}{0.5\rho U^2 Ld}, \tag{7}$$

$$C_L = \frac{F_L}{0.5\rho U^2 Ld}, \tag{8}$$

$$C_M = \frac{M}{0.5\rho U^2 Ld^2}, \tag{9}$$

where, C_D is Drag Coefficient; C_L is Lift Coefficient; C_M is Moment Coefficient; U is the

wind speed; ρ is the air density; L is the effective length of conductor; d is the effective width of the conductor to face the wind, in this paper, d is equal to D .

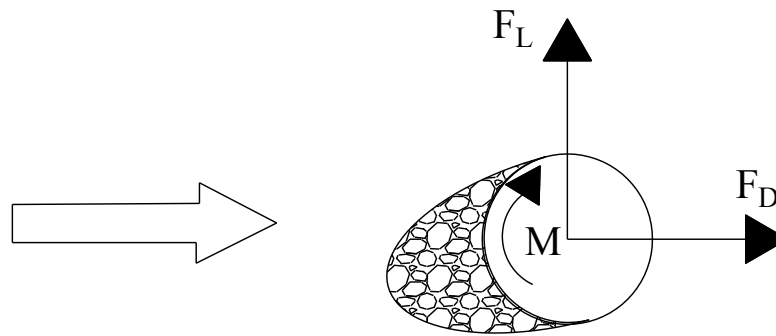


Figure 3. The direction of three component force coefficient.

3.6 The results of iced single conductor with crescent-section

For an iced single conductor with a crescent-section, the aerodynamic coefficients which were influenced by wind attack angle were obtained. As shown in Figure 4~6, the numerical simulation of aerodynamic coefficients was in accordance with wind tunnel test at Zhejiang University.

Figure 4 shows that the curve of the lift coefficient (C_L) was changed due to the wave transformation process. The Lift coefficient was close to zero with

an attack angle of 0° , 90° , 180° . The lift coefficient curve reached a positive peak at 20° and 170° . A negative peak appeared at 125° . As shown in Figure 5, the drag coefficient curve looked like a half wave shape, which was low at both ends but high at intermediate. The maximum drag coefficient appeared at 90° , while the minimum drag coefficient at 0° and 180° . It illustrated that the windward area was at maximum when the wind attack angle was 90° , and at the minimum when the windward area appeared at 0° and 180° .

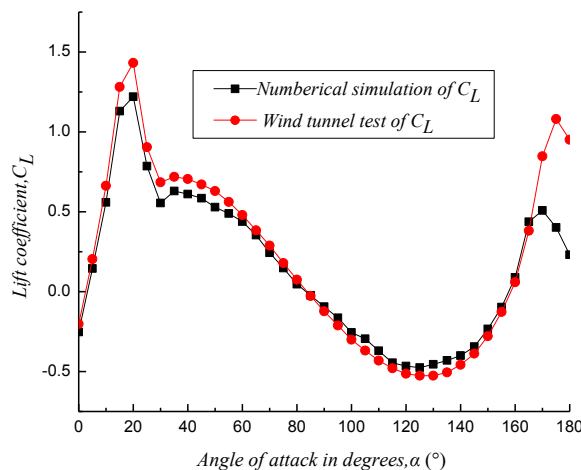


Figure 4. Lift coefficient of the iced single conductor with a crescent section.

As shown in Figure 6, the curve of the moment coefficient showed as a half wave shape, which was also low at both ends but high at intermediate. The maximum moment coefficient appeared at 130° and the value was 0.623. When the wind attack angles were 0°, 30°, 170°, the moment coefficient was close to zero, and the negative value appeared from 170° to 180°. The derivation of lift coefficient to wind attack angle was substituted into Equation (1), and the curve of Den. Hartog can be obtained, shown in Figure 7. The galloping of the iced single conductor with a crescent section was judged by Den. Hartog

mechanism. The coefficient of Den. Hartog was less than zero when the wind attack angles were between 10°~30° and 170°~180°, respectively, which indicated that the iced single conductor with a crescent section occurred to gallop easily in these scopes. The Nigol coefficient was the derivation of the moment coefficient to wind attack angle. As shown in Figure 8, when the wind attack angles were between 10°~30° and 110°~180°, the coefficients of Nigol were negative, according to the Nigol mechanism, Torsional galloping was prone to happen in these two regions.

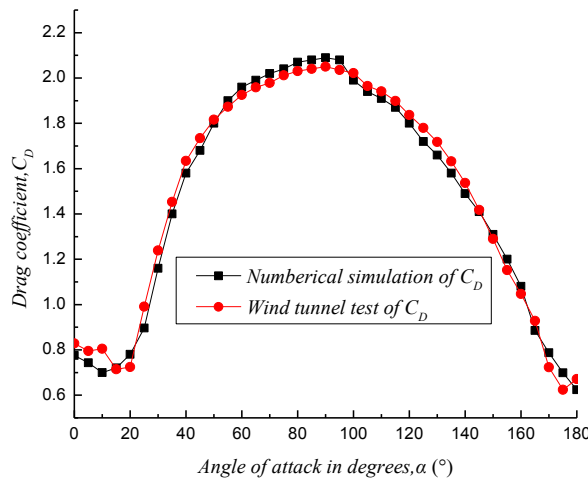


Figure 5. Drag coefficient of the iced single conductor with a crescent section.

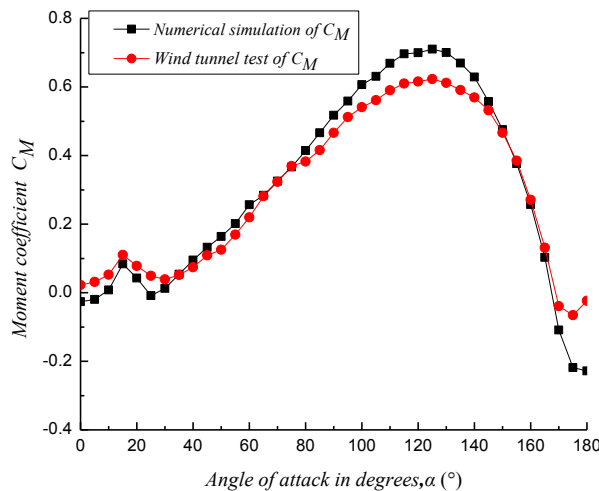


Figure 6. Moment coefficient of the iced single conductor with a crescent section.

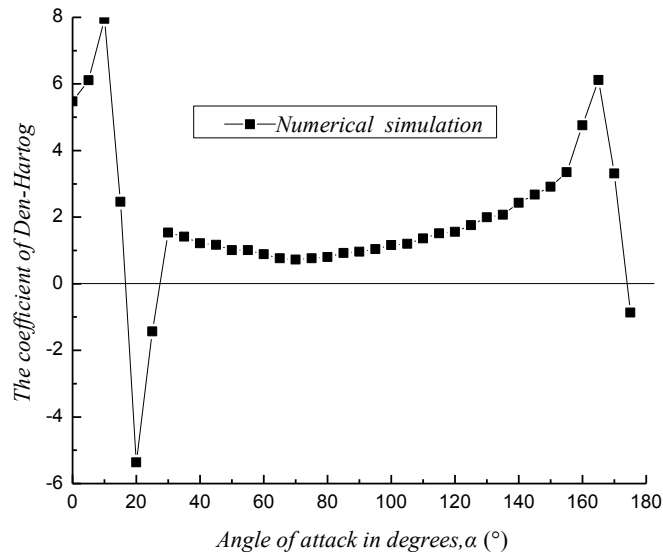


Figure 7. The coefficient of Den. Hartog of the iced single conductor with a crescent section.

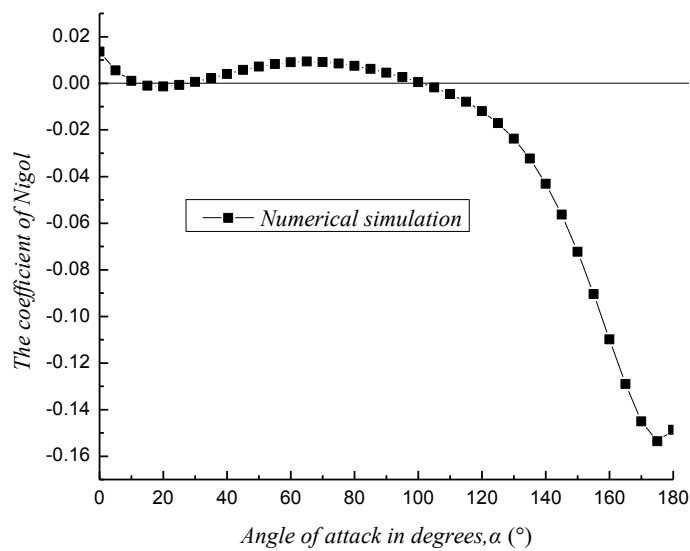


Figure 8. The coefficient of Nigol of the iced single conductor with a crescent section.

4 The wake of vortex shedding for the iced single conductor at 90° (wind attack angle)

The iced conductor was in the subcritical condition, and the wake of the iced conductor appeared in Karman vortex street. The calculation formula of Vortex shedding frequency was (Eq.10):

$$f_v = \frac{StU}{B}, \quad (10)$$

where, U is the wind speed; B is the reference length; St is the Strouhal number; for the iced conductor with the crescent section, St is 0.2.

Vortex shedding induced by a lateral flow was one of the reasons for vibration. For the subsonic velocity flow, when it flowed through the iced conductor, the back of the iced conductor appeared in Karman vortices, which was similar to a single cylindrical object. In this paper, for the iced conductor with a crescent section at 90° (wind attack angle), the whole process of the wake of vortex shedding was researched. Figure 9 gave a few representative moments of vortex shedding when the wind blew. The stable vortex street was formed by the alternate shedding vortex behind both sides of the conductor, which produced the periodic lift and drag.

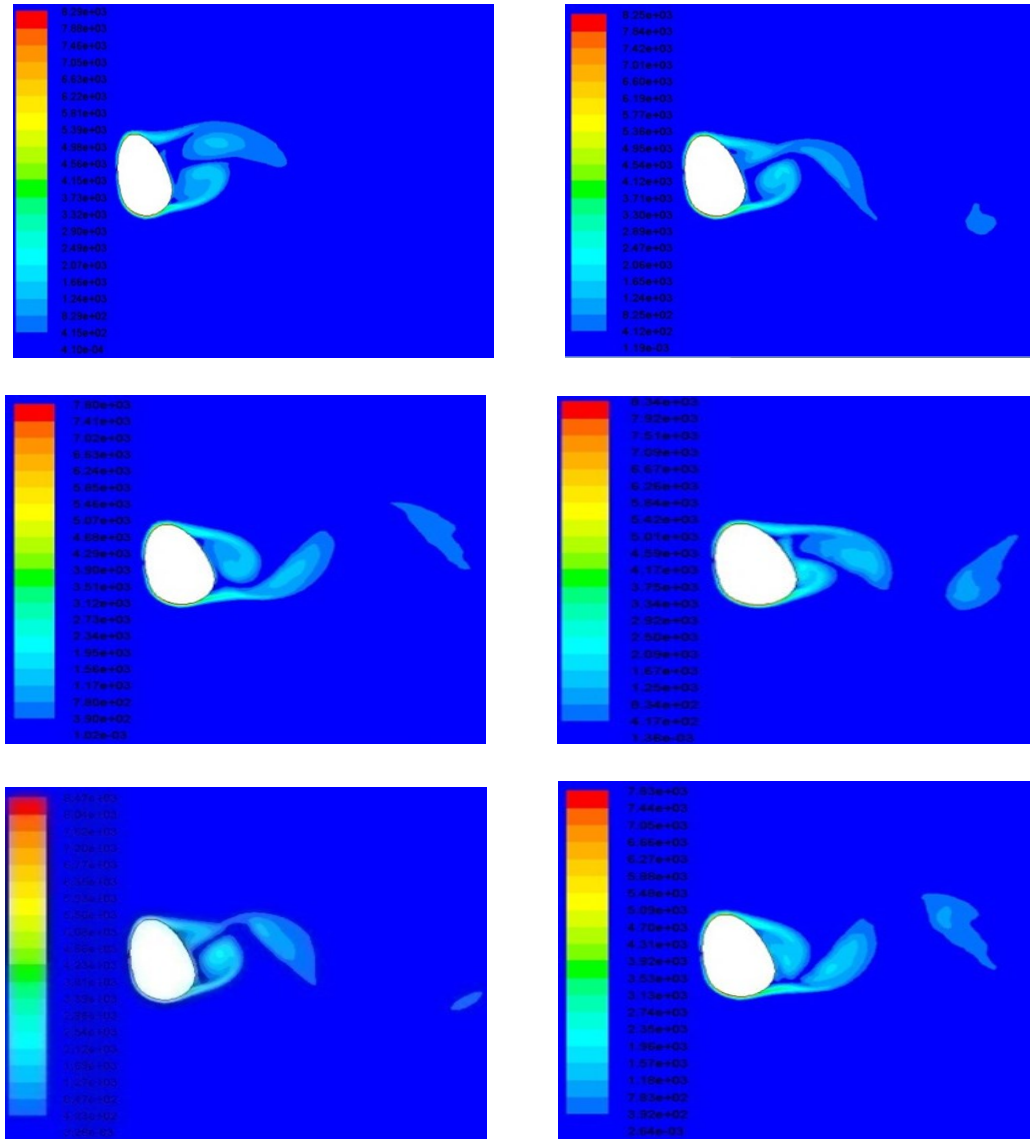


Figure 9. The change of vortex street for the iced conductor with a crescent section.

The pressure distribution was changed by the variation of streamline pattern, which can change the size and direction of fluid pressure acting on the iced conductor. Finally, the iced conductor began to vibrate.

5 Numerical simulation on aerodynamic characteristics of the iced bundled conductor with a crescent section

The natural ice accretion may be different on each conductor and one conductor may act as a damper while the other one alone would experience severe galloping, provided the both ends of sub-conductors in each sub-spans were fixed by spacers. It was difficult to reverse it when ice made the conductor be eccentric. Torsional stiffness was significantly higher than in the same section of the single conductor. The numerical model of iced bundled conductors was similar to a single conductor; the distance between two sub-conductors was 400mm, and the definition of the wind attack angle was illustrated as shown in Figure 10.

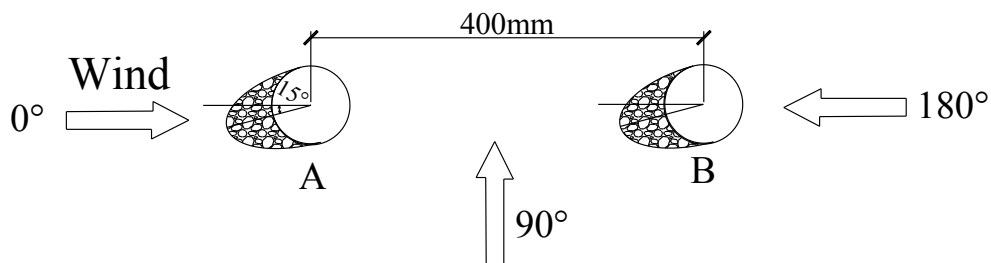


Figure 10. The modal of the twin bundled conductors with a crescent section.

When the wind attack angle was 90° , the windward of the two sub-conductors was very different, the shape of sub-conductor A to the windward appeared to be round, the windward side of sub-conductor B is elliptic so that aerodynamic coefficients of the two sub-conductors were very different at the 90° . The shape of cross-section has great influence on the aerodynamic coefficient.

It is worth noting that the transmission conductors used in the tests are multi-strands, the ice shape along the conductor was not the same, the model for simulation was simplified, and only a crescent typical ice shape was chosen to simulate the iced transmission lines. Its surface was smooth, and the roughness of the surface had a certain influence on

the aerodynamic coefficients. There were also some errors in using the CFD technique for solving the turbulence. Besides, all of the above factors brought about some differences in the results of numerical simulation and experiment, but these results, however, were very accurate and reasonable, and can be still used to describe and explore the aerodynamic characteristics of crescent iced conductors.

For the twin bundled conductors with crescent sections, the curve of three aerodynamic coefficients of sub-conductors at upstream and downstream locations were calculated for different wind attack angles. The influence of each sub-conductor was considered, and the results were shown in Figure 11 ~ Figure 13. Compared to the iced single conductor, the aerodynamic coefficients were changed due to wake-flow-influence of subconductors. When the wind attack angle was from 0° to 90° , sub-conductor A was in the upstream flow, and the aerodynamic force of sub-conductor A was larger than B. In the region of $90^\circ \sim 180^\circ$, sub-conductor B was in the upstream flow, the windward area of B was increased, and the aerodynamic parameter was larger than A. It was obvious that three aerodynamic coefficients of sub-conductor A changed suddenly when the wind attack angle was 90° . The ice changed the cross section of conductor, and the center of gravity of the iced conductor was shifted. The change of initial wind attack angle made the influence of sub-conductors more complicated.

the aerodynamic coefficients. There were also some errors in using the CFD technique for solving the turbulence. Besides, all of the above factors brought about some differences in the results of numerical simulation and experiment, but these results, however, were very accurate and reasonable, and can be still used to describe and explore the aerodynamic characteristics of crescent iced conductors.

The Den. Hartog coefficient of the twin bundled conductor with a crescent section was shown in Figure 14. The change was almost equal to the single conductor. With attack angles of $30^\circ \sim 40^\circ$ and $175^\circ \sim 180^\circ$, the coefficient by Den. Hartog was negative.

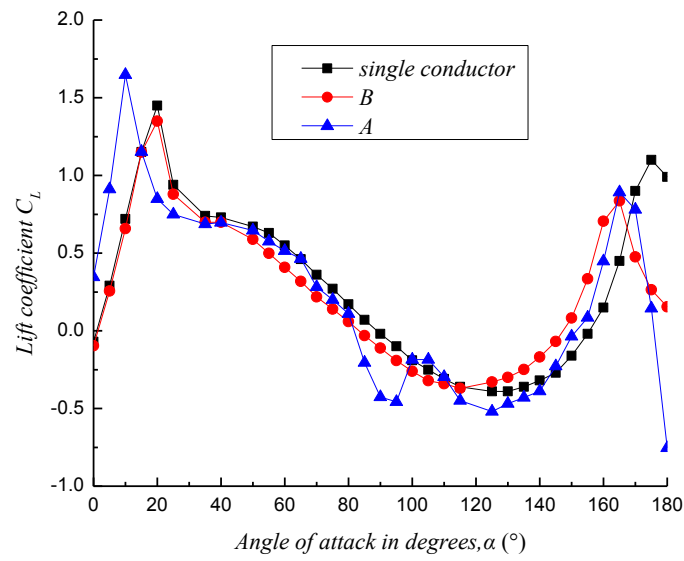


Figure 11. Lift coefficient of twin bundled conductors with crescent sections.

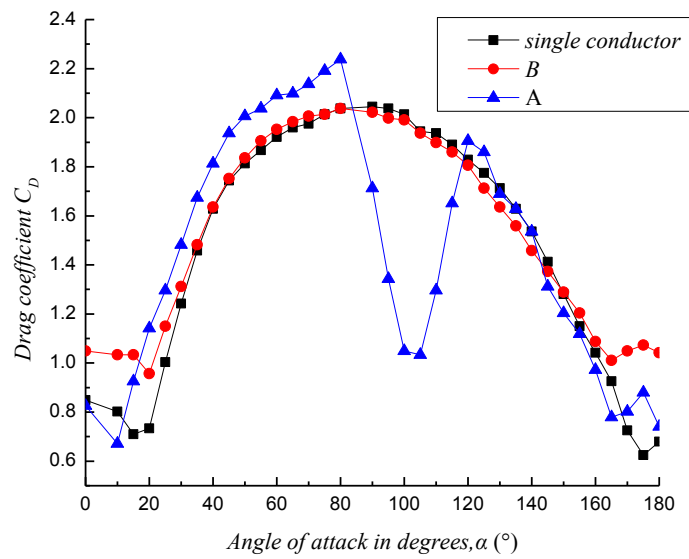


Figure 12. Drag coefficient of twin bundled conductors with crescent sections.

The maximum negative value appeared at 32°. According to Den. Hartog mechanism, twin bundled conductors with crescent sections were easily to gallop during these two regions. As shown in Figure 15, Nigol coefficients were negative with attack angles of 20°~25°, 75°~95° and 130°~165°. Compared with the single conductor, the negative

scope of the Nigol coefficients was larger than that of a single conductor. It can be concluded that bundled conductors were more likely to gallop than single ones, but the amplitude of galloping was found to be less than produced by a single conductor.

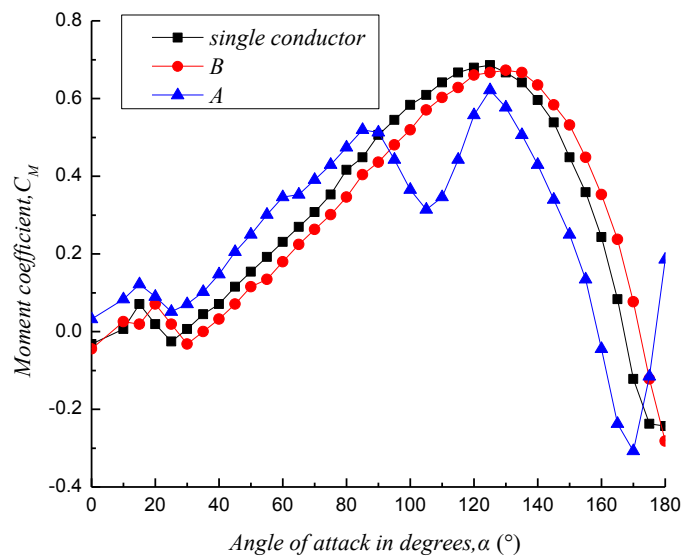


Figure 13. Moment coefficient of twin bundled conductors with crescent sections.

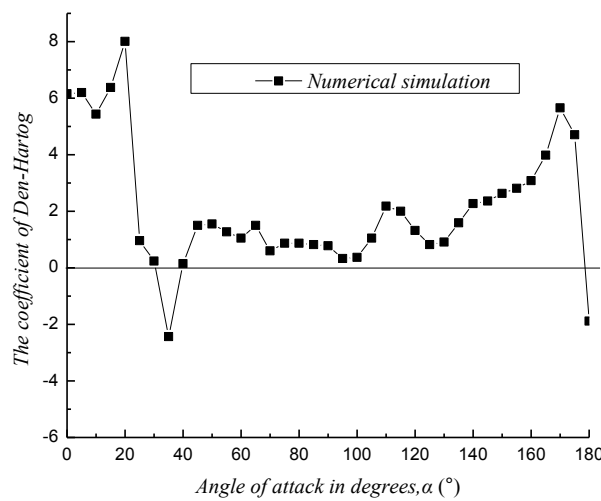


Figure 14. The Den. Hartog coefficient of the twin bundled conductor with a crescent section.

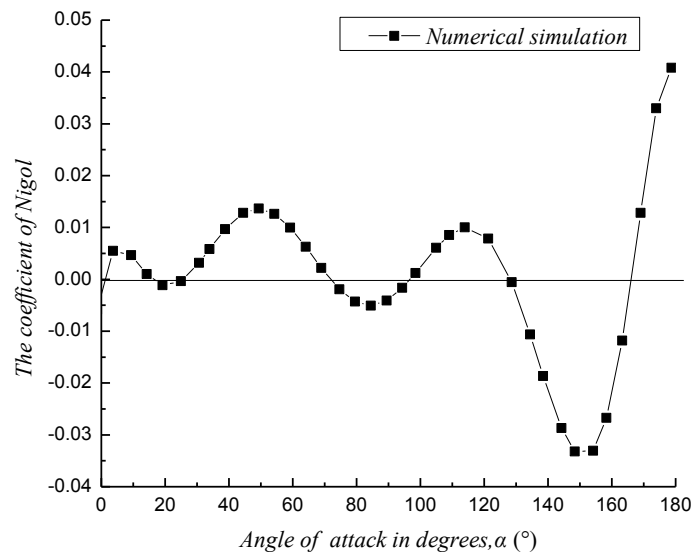


Figure 15. The Nigol coefficient of twin bundled conductor with crescent section.

6 Conclusion

Based on the numerical simulation and wind tunnel test, the galloping mechanism of iced conductors and the aerodynamic characteristics have been studied in this paper and some innovative and valuable conclusions (have been) reached as follows: (1) A new innovative numerical experiment and analysis method on aerodynamic characteristics of a single conductor and bundled conductors with typical ice-coating sections were referred to in this paper. Compared with the results from the wind tunnel test at Zhejiang University, the numerical results agreed with the wind tunnel test very well, pointing out that this new method was more reliable and more high-effective than those of the present general numerical analyzing methods.

(2) The Den. Hartog and Nigol coefficients were calculated at a given wind speed, which can be used to predict the galloping for most of the wind conditions.

(3) For the iced conductor with a crescent section at 90° (wind attack angle), the stable vortex street was formed by the alternate shedding vortex behind both sides of the conductor, which produced the periodic lift and drag. The pressure distribution varied according to the streamline pattern, which caused the changes of the size and direction of the fluid

pressure acting on the iced conductor.. Finally, the iced conductor began to vibrate.

(4) The model of twin bundled conductors with a crescent section was built up, three aerodynamic coefficients of the iced twin bundled conductor with a crescent section were calculated at different wind attack angles. The influence of each sub-conductor was considered. Compared with the iced single conductor, the aerodynamic parameters of bundled conductors were influenced by the wake of sub-conductors. The ice changed the cross section of the conductor, and the gravity center of the iced conductor was shifted. The changes of initial wind attack angles made the influence from sub-conductors much more complicated.

References

- [1] Chabart, O., Lilien, J. L.: *Galloping of electrical lines in wind tunnel facilities*, Journal of Wind Engineering and Industrial Aerodynamics, 74-76 (1998), 967-976.
- [2] Yan, Z., Li, Z., Savory, E., et al. : *Galloping of a single iced conductor based on curved-beam theory*, Journal of Wind Engineering and Industrial Aerodynamics, 123(2013), 77-87.
- [3] Yan, Z., Savory, E., Li, Z. et. al.: *Galloping of iced quad-conductors bundles based on curved*

- beam theory*, Journal of Sound and Vibration, 333 (2014), 1657-1670.
- [4] Loredo-Souza, A. M., Davenport, A. G.: *A novel approach for wind tunnel modeling of transmission lines*, Journal of Wind Engineering and Industrial Aerodynamics, 89 (2001), 1017–1029.
- [5] Xie, Q., Sun, Q. Guan, Z. et. al.: *Wind tunnel test on global drag coefficients of multi-bundled conductors*, Journal of Wind Engineering and Industrial Aerodynamics, 120(2013), 9-18.
- [6] Van Dykea, P., Laneville, A.: *Galloping of a single conductor covered with a D-section on a high-voltage overhead test line*, Journal of Wind Engineering and Industrial Aerodynamics, 96 (2008), 1141–1151.
- [7] Loredo-Souza, A. M., Davenport, A. G.: *Wind tunnel aeroelastic studies on the behaviour of two parallel cables*, Journal of Wind Engineering and Industrial Aerodynamics, 90 (2002), 407–414.
- [8] Yinglong, G., Lili, Y., Wujun, B. et. al.: *Study on the Galloping of Overhead Transmission Line*, J.Wuhan Univ. of Hydr. & Elec.eng, 28(1995), 5, 506-509.
- [9] Junqing, Y., Yinglong, G., Xiaohui, X.: *Computer simulation of power line galloping*, Engineering Journal of Wuhan University, 35(2002), 1, 40-43.
- [10] Wanping, L., Huang, H., Zeng, H.: *Aerodynamic Characteristics of Heavily Iced Conductors*. J.Huazhong Univ. of sci. & Tech. 29(2001), 8, 84-86.
- [11] Den Hartog, J. P.: *Mechanical vibrations (second edition)*, NewYork: McGraw-Hill Book Company
- [12] Nigol, O., Clarke, G. J.: *Conductor galloping and control based on torsional mechanism*, NewYork IEEE Power Engineering Society Winter Meeting, 1974.
- [13] Nigol, O., Buehan, P. G.: *Conductor Galloping PartI-Den Hardog Mechanism*, IEEE Trans.On Power Apparatus and Systems, 100(1981), 5, 699-707.
- [14] Xin, W.: *Wind Tunnel Test on Galloping of Iced Conductors and Galloping Simulation for Transmission Tower-Line System*, Zhe Jiang University, Zhejiang, China.
- [15] Alonso, G., Meseguer, J. : *A parametric study of the galloping stability of two-dimensional triangular cross-section bodies*, Journal of Wind Engineering and Industrial Aerodynamics 94 (2006), 241-253.

